

# Peculiar electrochemical behaviors of $(1 - x)\text{LiNiO}_2 \cdot x\text{Li}_2\text{TiO}_3$ cathode materials prepared by spray drying

Lianqi Zhang, Takahisa Muta, Hideyuki Noguchi<sup>\*</sup>, Xiaoqing Wang, Meijing Zhou, Masaki Yoshio

*Department of Applied Chemistry, Saga University, Saga 840-8052, Japan*

Received 10 October 2002; accepted 27 January 2003

## Abstract

The cathode materials,  $(1-x)\text{LiNiO}_2 \cdot x\text{Li}_2\text{TiO}_3$  with  $0.05 \leq x \leq 0.5$ , were first prepared by a spray drying route. The XRD results indicated that co-substituting Li and Ti for Ni in  $\text{LiNiO}_2$  contributes to increasing cations disorder in the materials. Charge–discharge tests in the voltage range of 3.0–4.4 V exhibited expected results: the more simple charge–discharge curves, the decreased capacity and the increased Columbic irreversibility with increasing  $x$ . However, when charged up to 4.8 V, the materials with  $x \geq 0.075$  surprisingly presented unusual electrochemical properties, an excess charge capacity beyond the oxidization of  $\text{Ni}^{3+}$  to  $\text{Ni}^{4+}$  in materials with the presence of a charge plateau at about 4.5–4.7 V during the initial cycle. These phenomena are very similar to those reported in  $(1-y)\text{LiNi}_{0.5}\text{Mn}_{0.5}\text{O}_2 \cdot y\text{Li}_2\text{MnO}_3$  [J. Electrochem. Soc. 149 (2002) A815]. The sample with  $x = 0.05$  indicated promising electrochemical properties in term of capacity and cyclability even charged to 4.8 V.

© 2003 Elsevier Science B.V. All rights reserved.

**Keywords:** Peculiar electrochemical behaviors;  $(1-x)\text{LiNiO}_2 \cdot x\text{Li}_2\text{TiO}_3$ ; Cathode materials; Spray drying; Cations disorder

## 1. Introduction

The layered  $\text{LiNiO}_2$  is an attractive cathode material for lithium ion batteries with its relatively low cost and high capacity [1]. However,  $\text{LiNiO}_2$  is also known for some problems like being difficult to prepare excellent electro-active materials due to stoichiometric deviation, poor cycling property when it is charged to a higher voltage [2] (4.3 V versus  $\text{Li}^+/\text{Li}$ ) as well as its well-known safety concern [3]. Various attempts have addressed the above problems by foreign cations substitution for Ni or surface modification.

Recently, stabilizing layered cathode materials like  $\text{LiNiO}_2$  [4,5],  $\text{LiCoO}_2$  [6,7],  $\text{LiFeO}_2$  [8,9] or  $\text{LiCrO}_2$  [10–12] based on  $\text{LiAO}_2 \cdot \text{Li}_2\text{MO}_3$  ( $A = \text{Ni}, \text{Co}, \text{Cr}, \text{Fe}$  and  $M = \text{Mn}, \text{Ti}$ ) solid solution, corresponding to co-substitute Li and M for A in  $\text{LiAO}_2$ , has drawn more and more attention. We have reported the effect of stabilizing  $\text{LiNiO}_2$  by a solid solution with  $\text{Li}_2\text{MnO}_3$  in a wide range [5].  $\text{Li}_2\text{TiO}_3$  [13] has a same layered structure as  $\text{Li}_2\text{MnO}_3$

[14], but Ti is lighter and has a redox state at a lower potential of <3 V as well as the stronger bonding capability with O compared with Mn.  $\text{Li}_2\text{TiO}_3$  has been reported to be capable of stabilizing the structure of layered  $\text{LiNi}_{0.5}\text{Mn}_{0.5}\text{O}_2$  [15,16] and  $\text{LiCrO}_2$  [12]. Further,  $\text{LiNiO}_2$  with Ti doping has been claimed to have the highest capacity and best electrochemical reversibility among the known layered materials [17,18] as well as the significant improvement of thermal stability [19]. In addition, it was pointed out that the homogeneity of materials at microscopic scale is crucial to obtain excellent performance for doped  $\text{LiNiO}_2$  [20]. However, to our best knowledge, cathode materials with Ti doping, which are prepared by a way favorable to get homogenous phase instead of conventional solid-state route, were not reported so far.

In this work,  $(1-x)\text{LiNiO}_2 \cdot x\text{Li}_2\text{TiO}_3$  ( $0.05 \leq x \leq 0.5$ ) solid solution was first successfully prepared via a homogenous precursor obtained by spray drying method. Structural disorder trend of materials with the increase of Ti content was identified, but some peculiar and interesting electrochemical behaviors, similar to those reported by Lu and Dahn [21] and Lu et al. [22], were observed and provided valuable information on understanding electrochemical reaction mechanism of materials.

<sup>\*</sup> Corresponding author. Tel.: +81-952-28-8674; fax: +81-952-28-8591.  
E-mail address: [noguchih@cc.saga-u.ac.jp](mailto:noguchih@cc.saga-u.ac.jp) (H. Noguchi).

## 2. Experimental

Materials were prepared by the following method. Stoichiometric  $\text{LiOH}\cdot\text{H}_2\text{O}$ ,  $\text{Ni}(\text{CH}_3\text{COO})_2\cdot 4\text{H}_2\text{O}$  and titanium coating solution (the acidic solution of  $[\text{NH}_4]_2[\text{Ti}(\text{C}_2\text{O}_4)_3]$ ) (TKC-305, Tayca Co.) were dissolved in water with the aid of citric acid. The transparent solution was fed into a spray drying instrument (pulvis mini-spray GB22, Yamato, Japan) to produce a homogenous precursor (electron-probe micro-analysis (EPMA) has been performed to confirm the homogeneity of the precursor at molecular scale). The precursor was initially decomposed at  $400\text{ }^\circ\text{C}$  in air and then ground after cooling. The decomposed mixture was pelletized under  $1000\text{ kg/cm}^2$  and, finally, calcined at  $750\text{ }^\circ\text{C}$  in  $\text{O}_2$  for 15 h. Samples were ground again after cooling and then kept in a desiccator with blue silica-gel.

The crystallographic properties of samples were characterized using a Rigaku diffractometer (RINT 1000) with  $\text{Cu K}\alpha$  radiation. The elemental analysis of lithium, nickel and titanium in the materials was conducted using an inductively coupled plasma spectrometer (ICP, SPS 7800, Seiko Instruments, Japan).

The charge and discharge characteristics of Li–Ni–Ti–O cathodes were examined in CR2032 coin-type half-cell (Li/Li–Ni–Ti–O). Cells were composed of a cathode and a lithium metal anode (Cyprus Foote Mineral Co.) separated by a porous polypropylene film (Celgard 3401) and two glass fiber mats. The cathode consisted of 20 mg active material and 12 mg conductive binder (8 mg polytetrafluoroethylene (PTFE) and 4 mg acetylene black). It was pressed on a stainless steel mesh at  $800\text{ kg/cm}^2$  and then dried in vacuum at  $150\text{ }^\circ\text{C}$  for 6 h. The electrolyte solution was a 1:2 mixture of ethylene carbonate (EC) and dimethylcarbonate (DMC) containing 1 M  $\text{LiPF}_6$ . All cells were assembled in

an argon-filled dry box. Cells were typically cycled in the voltage range of 3.0–4.4 and 3.0–4.8 V at a constant current density of  $0.23\text{ mA/cm}^2$  ( $20\text{ mA/g}$ ).

## 3. Results and discussion

Fig. 1 shows the XRD patterns of several samples. Typical miller indices based on hexagonal lattice are also shown in the figure. All samples can be identified as a pure phase. The intensity ratio of (0 0 3) versus (1 0 4) peaks in hexagonal unit cell gradually decreases with the increasing  $x$  and, in the case of  $x = 0.5$ , several peaks such as (0 0 3), (1 0 1), etc. basically disappear, which means that the increase of Ti content causes a gradual transformation from layered structure to rock-salt structure; especially for  $x = 0.5$  the structure has become a completely disorder rock-salt one. The change in the intensity ratio of (0 0 3) versus (1 0 4) peaks together with that in hexagonal lattice parameters,  $a$  and  $c$ , and unit cell volume is illuminated in Fig. 2 (for convenience of comparison, cubic lattice parameter was converted to hexagonal one according to the equation of  $a_h = (\sqrt{2}/2)a_c$  and  $c_h = 2\sqrt{3} \times a_c$ ). Lattice parameters,  $a$  and  $c$ , increase with increasing  $x$  value and, hence, result in the increase of unit cell volume, although the intensity ratio of peak (0 0 3) against peak (1 0 4) in hexagonal unit cell gradually decreases. The XRD results demonstrate that Li and Ti atoms co-substituted for Ni in  $\text{LiNiO}_2$  have the nature of accelerating the 3d cations disorder in the layered materials.

Table 1 shows the results of elemental analysis for  $(1-x)\text{LiNiO}_2\cdot x\text{Li}_2\text{TiO}_3$  ( $0.05 \leq x \leq 0.5$ ). Results indicate little deviation in the atomic ratio of three metal elements, Li, Ni and Ti, from the aimed values for all samples. Therefore, the obtained materials should be based on the

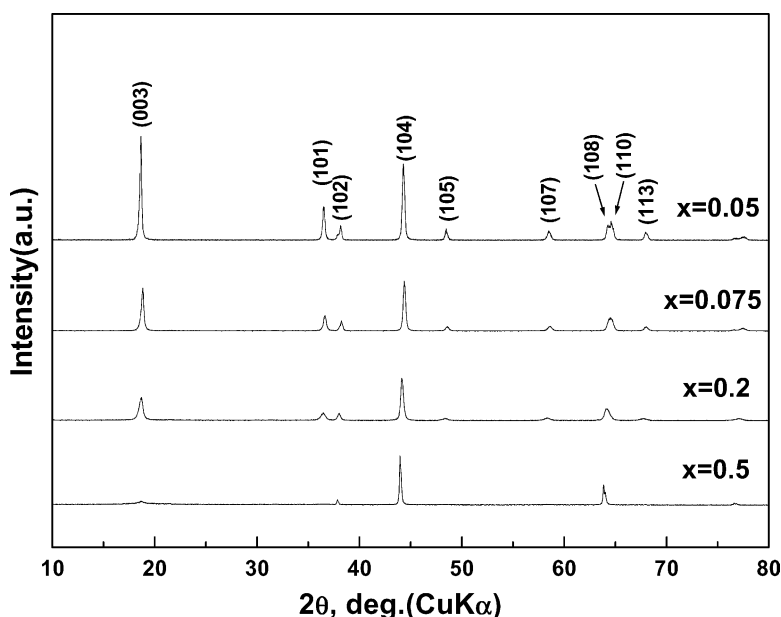


Fig. 1. The XRD patterns for several typical samples in  $(1-x)\text{LiNiO}_2\cdot x\text{Li}_2\text{TiO}_3$ .

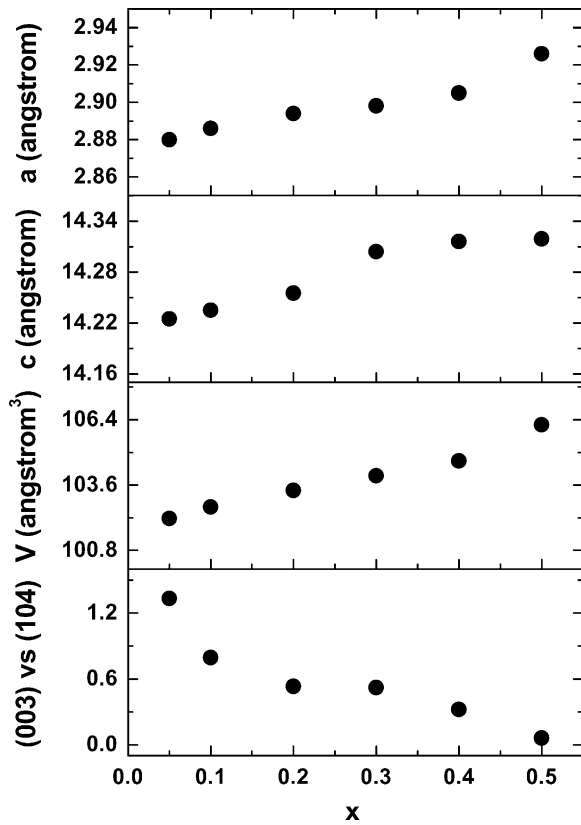


Fig. 2. Lattice parameters, unit cell volume and the intensity ratio of (003) versus (104) peaks in hexagonal unit cell for  $(1-x)\text{LiNiO}_2 \cdot x\text{Li}_2\text{TiO}_3$ .

solid solution between  $\text{LiNiO}_2$  and  $\text{Li}_2\text{TiO}_3$ . If a certain error is considered during the elemental analysis experiment, the formula of  $(1-x)\text{LiNiO}_2 \cdot x\text{Li}_2\text{TiO}_3$  ( $0.05 \leq x \leq 0.5$ ) might be used as the compositional representation for all samples, which can be also rewritten as  $\text{Li}_{1+x}\text{Ni}_{1-x}^{3+}\text{Ti}_x^{4+}\text{O}_{2+x}$ , and further  $\text{Li}[\text{Li}_{x/(2+x)}\text{Ni}_{(2-2x)/(2+x)}\text{Ti}_{2x/(2+x)}]\text{O}_2$  provided that the materials have the ideal layered structure.

Charge–discharge curves for these samples are indicated in Fig. 3. When cells are cycled in the voltage range of 3.0–4.4 V; as expected, the complex  $\text{LiNiO}_2$ -type

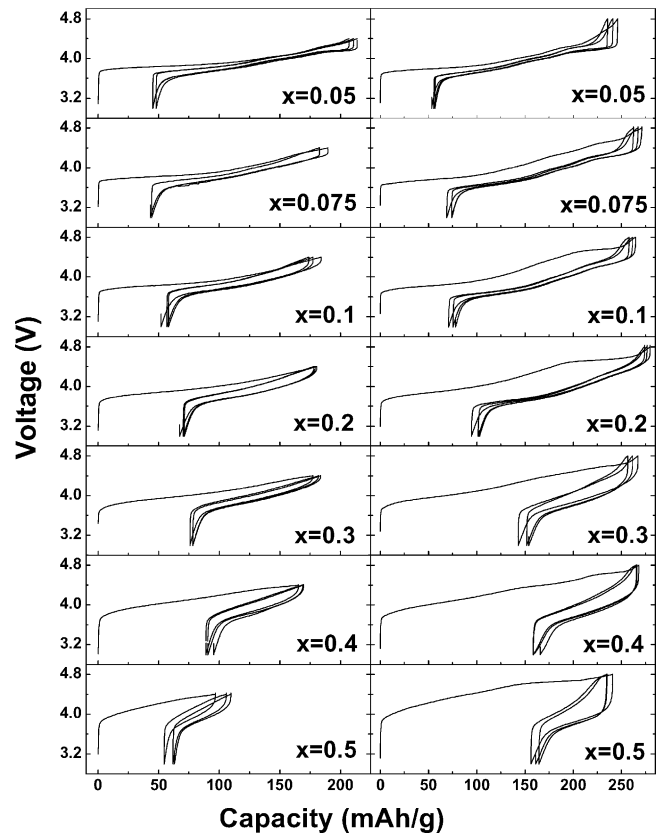


Fig. 3. Charge–discharge curves of  $(1-x)\text{LiNiO}_2 \cdot x\text{Li}_2\text{TiO}_3$  cells cycled in the voltage range of 3.0–4.4 V (left panel) and 3.0–4.8 V (right panel) at a constant current density of  $0.23 \text{ mA/cm}^2$  (20 mA/g).

charge–discharge curves are progressively displaced by more simple ones as same as Mn doped lithium nickelates [5], initial charge–discharge capacities gradually decrease and Columbic irreversibility except for  $x = 0.5$  gradually increases with the increasing  $x$ . These can be all explained by cations disorder in the Ti doped materials. However, when cells are operated in the voltage range of 3.0–4.8 V, samples except for  $x = 0.05$ , surprisingly present some unusual electrochemical behaviors. The initial charge capacity for the samples with  $x \geq 0.075$  exceeds the calculated capacity (CC1) based on the assumption that Ni is trivalent state, Ti is tetravalent state, and thereby only  $\text{Ni}^{3+}$  can be oxidized to  $\text{Ni}^{4+}$  in materials (see Eq. (1)). Fig. 4 summarized the charge–discharge capacities for all samples together with their calculated capacity lines CC1 and CC2. CC2 is calculated provided that samples have ideal layered structure and  $\text{Li}^+$  in Li layers can be completely extracted (see Eq. (2)). CC1 and CC2 can be described as the following two Eqs. (1) and (2), respectively:

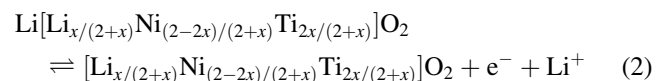
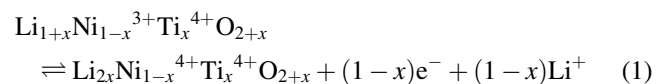


Table 1  
Elemental analysis data of  $(1-x)\text{LiNiO}_2 \cdot x\text{Li}_2\text{TiO}_3$

Samples ( $x$ )	Metal ions chemical composition		
	Li	Ni	Ti
0.05	1.060	0.984	0.05
0.075	1.076	0.940	0.075
0.1	1.080	0.863	0.1
0.2	1.195	0.790	0.2
0.3	1.270	0.690	0.3
0.4	1.386	0.592	0.4
0.5	1.480	0.493	0.5

Fixing Ti content as the targeted value as indicated in  $(1-x)\text{LiNiO}_2 \cdot x\text{Li}_2\text{TiO}_3$  ( $0.05 \leq x \leq 0.5$ ).

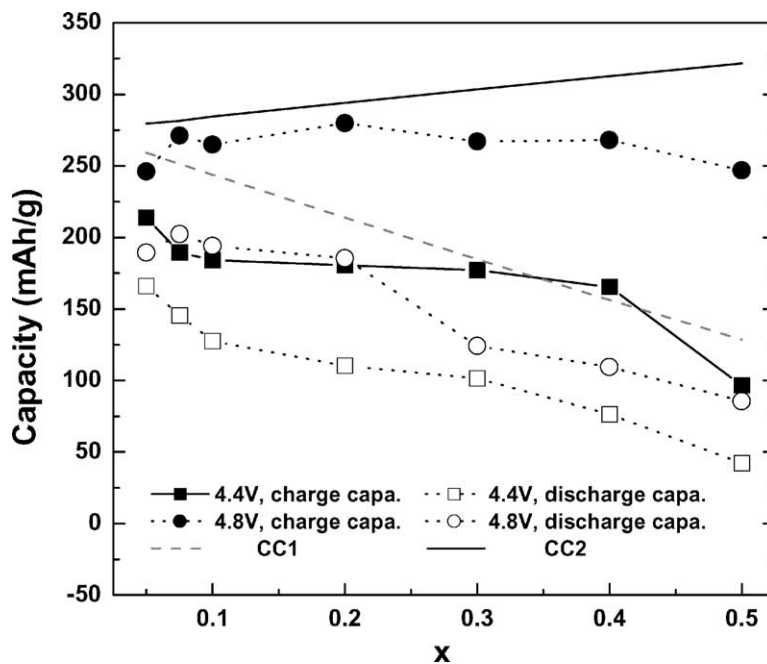


Fig. 4. Initial charge–discharge capacity of  $(1-x)\text{LiNiO}_2 \cdot x\text{Li}_2\text{TiO}_3$  as well as their calculated capacity: CC1 and CC2. CC1 is calculated assuming that Ni is trivalent state, Ti is tetravalent state, and thereby only  $\text{Ni}^{3+}$  can be oxidized to  $\text{Ni}^{4+}$  in materials; while CC2 is derived provided that samples have ideal layered structure and  $\text{Li}^+$  in Li layers can be completely extracted.

It is found that the initial charge capacity of the samples, except for  $x = 0.05$ , for cycling in the voltage range of 3.0–4.8 V lies between the two calculated capacity lines, CC1 and CC2, while the initial charge capacity for cycling in the voltage range of 3.0–4.4 V and all discharge capacities are located below the calculated capacity line, CC1.

Excess initial charge capacity beyond oxidization of  $\text{Ni}^{3+}$  to  $\text{Ni}^{4+}$ , in general, is conventionally explained by decomposition of electrolyte. However, some other peculiar electrochemical behaviors to be discussed in the following during charge–discharge processes suggest that such an explanation is possibly unsuitable. As indicated in the right panel of Fig. 3, samples with  $x \geq 0.075$ , especially for  $x = 0.1, 0.2$  and  $0.5$ , exhibit a clear long charge plateau at  $>4.5$  V during the initial cycle when cells are charged to 4.8 V. This becomes clear in their chronopotentiograms as shown in Fig. 5. Lu and Dahn [21] and Lu et al. [22] recently reported a very similar phenomenon in the  $(1-y)\text{LiNi}_{0.5}\text{Mn}_{0.5}\text{O}_2 \cdot y\text{Li}_2\text{MnO}_3$  cathode materials. They demonstrated through many evidences that simultaneous extraction of oxygen and lithium should account for the long charge plateau. Kim et al. also pointed out that the instability of  $\text{LiNi}_{0.5}\text{Mn}_{0.5}\text{O}_2$  related to oxygen loss is possibly responsible for the relatively lower Columbic efficiency [15]. In our experiments, more importantly, some samples ( $x = 0.075, 0.1$  and  $0.2$ ) present a very small charge–discharge polarization after initial charge to 4.8 V in contrast with that cycling in the voltage range of 3.0–4.4 V. As a result, it is unreasonable to ascribe the small polarization after charging to 4.8 V to electrolyte decomposition since electrolyte decomposition

on electrode surface generally does not reduce the charge–discharge polarization. Therefore, the excess charge capacity associated with the charge plateau possibly results mainly from simultaneously removing Li and O from structure under the condition that  $\text{Ni}^{4+}$  and  $\text{Ti}^{4+}$  are very difficult or impossible to be oxidized to a higher valence, as concluded in the  $(1-y)\text{LiNi}_{0.5}\text{Mn}_{0.5}\text{O}_2 \cdot y\text{Li}_2\text{MnO}_3$  cathode materials [21]. The further confirmation needs to be carried out and some experiments are also under the process in our lab. In addition, some other change in Figs. 3 and 5 can be observed. One, similar to that observed in the  $(1-y)\text{LiNi}_{0.5}\text{Mn}_{0.5}\text{O}_2 \cdot y\text{Li}_2\text{MnO}_3$  cathode materials [21,22], is that charge–discharge voltage apparently becomes lower after initial charge to 4.8 V for the samples with  $x = 0.075–0.2$ . The other is that unusual electrochemical reactions for the samples with  $x = 0.3–0.5$  seem to occur earlier at the voltage lower than 4.5 V. The capacity of the sample with  $x = 0.4$  exceeds the calculated capacity, CC1, even though cells are charged to 4.4 V.

The cyclability for samples under two kinds of voltage models are tested. All samples cycled in the voltage range of 3.0–4.4 V show viable cyclability at least until 50th cycle despite the degree of cations disorder, while for cycling in the voltage range of 3.0–4.8 V the samples with  $x = 0.05$  and  $0.3–0.5$  exhibit the stable cyclability after some capacity loss during initial several cycles. Consequently, the sample with  $x = 0.05$  indicates the best promising electrochemical properties in view of capacity and cyclability. Its cycling performance is shown in Fig. 6. Surprisingly, the cyclability in the voltage range of 3.0–4.8 V is superior to that in the voltage range of 3.0–4.4 V. The reason is not clear yet.

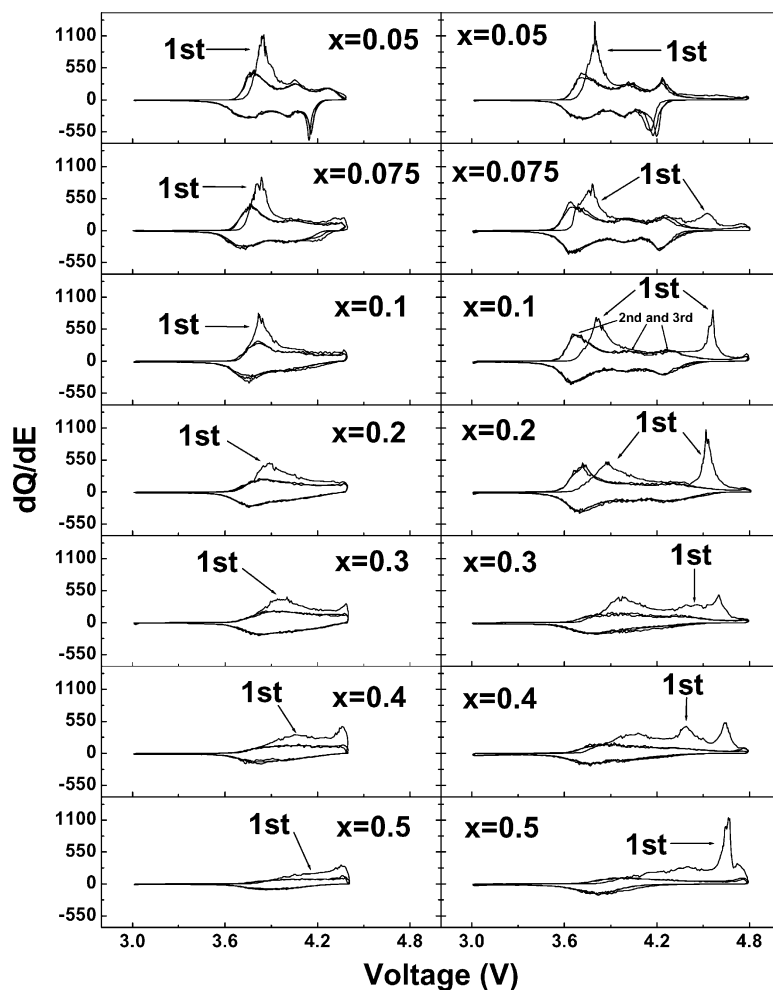


Fig. 5. Differential capacity vs. voltage for  $(1-x)\text{LiNiO}_2 \cdot x\text{Li}_2\text{TiO}_3$  cells cycled in the voltage range of 3.0–4.4 V (left panel) and 3.0–4.8 V (right panel) at a constant current density of  $0.23 \text{ mA/cm}^2$  ( $20 \text{ mA/g}$ ).

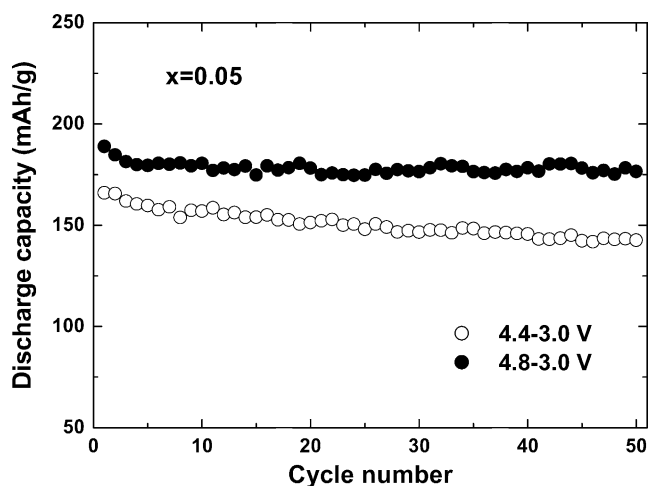


Fig. 6. Cycling performance of the sample with  $x = 0.05$  in the voltage range of 3.0–4.4 and 3.0–4.8 V at a constant current density of  $0.23 \text{ mA/cm}^2$  ( $20 \text{ mA/g}$ ).

#### 4. Conclusion

A spray drying route was developed to prepare the  $(1-x)\text{LiNiO}_2 \cdot x\text{Li}_2\text{TiO}_3$  ( $0.05 \leq x \leq 0.5$ ) solid solution. The XRD results showed that structure gradually becomes disorder with increasing  $x$ ; as  $x$  increases to 0.5, the sample possesses a completely disorder rock-salt structure. As charged to 4.4 V, samples exhibited the conventionally expected results; however, the samples with  $x \geq 0.075$  presented unusual electrochemical phenomena with upper voltage limitation of 4.8 V. A charge plateau at  $>4.5 \text{ V}$  was observed during the initial cycle and resulted in an excess charge capacity exceeding the calculated capacity based on the oxidization of Ni in samples. Furthermore, the larger the  $x$  value is, the more the excess charge capacity is. Subsequent small charge–discharge polarization for some samples after the initial long charge plateau suggested that the unusual electrochemical behaviors are possibly associated with the simultaneous removing lithium and oxygen from

structure of material, instead of electrolyte decomposition, as reported. Additionally, from the point of application the materials with low Ti content such as  $x = 0.05$  exhibited the viable capacity and cycling performance. Summarily, Li and Ti atoms co-doped into  $\text{LiNiO}_2$  do not play a favorable role in stabilizing the layered structure of  $\text{LiNiO}_2$  especially when  $x$  value exceeds 0.05 in  $(1-x)\text{LiNiO}_2 \cdot x\text{Li}_2\text{TiO}_3$ , and the larger the  $x$  value is, the more disorder and unstable the structure is.

## References

- [1] J.R. Dahn, U. von Sacken, C.A. Michal, *Solid State Ion.* 44 (1990) 87.
- [2] T. Ohuku, A. Ueda, M. Nagayama, *J. Electrochem. Soc.* 140 (1993) 1862.
- [3] J.R. Dahn, E.W. Fuller, M. Obrovac, U. von Sacken, *Solid State Ion.* 69 (1994) 265.
- [4] E. Rossen, C.D.W. Jones, J.R. Dahn, *Solid State Ion.* 57 (1992) 311.
- [5] L. Zhang, H. Noguchi, M. Yoshio, *J. Power Sources* 110 (2002) 57.
- [6] K. Numata, C. Sakaki, S. Yamanaka, *Chem. Lett.* 8 (1997) 725.
- [7] K. Numata, C. Sakaki, S. Yamanaka, *Solid State Ion.* 117 (1999) 257.
- [8] M. Tabuchi, H. Shigemura, K. Ado, H. Kobayashi, H. Sakaebe, H. Kageyama, R. Kanno, *J. Power Sources* 97–98 (2001) 415.
- [9] M. Tabuchi, A. Nakashima, H. Shigemura, K. Ado, H. Kobayashi, H. Sakaebe, H. Kageyama, T. Nakamura, M. Kohzaki, A. Hirano, R. Kanno, *J. Electrochem. Soc.* 149 (2002) A509.
- [10] C. Storey, I. Kargina, Y. Grincourt, I.J. Davidson, Y.C. Yoo, D.Y. Seung, *J. Power Sources* 97–98 (2001) 541.
- [11] M. Balasubramanian, J. Mcbreen, I.J. Davidson, P.S. Whitfield, I. Kargina, *J. Electrochem. Soc.* 149 (2002) A176.
- [12] L. Zhang, H. Noguchi, *Electrochem. Commun.* 4 (2002) 560.
- [13] T. Ohzuku, A. Ueda, N. Yamamoto, *J. Electrochem. Soc.* 142 (1995) 1431.
- [14] V. Massarotti, M. Bini, D. Capsoni, A. Altomare, A.G.G. Moliterni, *J. Appl. Crystallogr.* 30 (1997) 123.
- [15] J.-S. Kim, C.S. Johnson, M.M. Thackeray, *Electrochem. Commun.* 4 (2002) 205.
- [16] C.S. Johnson, J.-S. Kim, A.J. Kropf, A.J. Kahaian, J.T. Vaughey, M.M. Thackeray, *Electrochem. Commun.* 4 (2002) 492.
- [17] J. Kim, K. Amine, *Electrochem. Commun.* 3 (2002) 52.
- [18] J. Kim, K. Amine, *J. Power Sources* 104 (2002) 33.
- [19] H. Arai, S. Okada, Y. Sakurai, J. Yamaki, *J. Electrochem. Soc.* 144 (1997) 3177.
- [20] C. Delmas, M. Menetrier, L. Croguennec, I. Saadoune, A. Rougier, C. Pouillier, G. Prado, M. Grune, L. Fournes, *Electrochim. Acta* 45 (1999) 243.
- [21] Z. Lu, J.R. Dahn, *J. Electrochem. Soc.* 149 (2002) A815.
- [22] Z. Lu, L.Y. Beaulieu, R.A. Donaberger, C.L. Thomas, J.R. Dahn, *J. Electrochem. Soc.* 149 (2002) A778.